Atmos. Meas. Tech., 14, 2941–2955, 2021
https://doi.org/10.5194/amt-14-2941-2021

Atmospheric Measurement Techniques
Open Access
EGU

Two-dimensional monitoring of air pollution in Madrid using a Multi-AXis Differential Optical Absorption Spectroscopy two-dimensional (MAXDOAS-2D) instrument

David Garcia-Nieto[1,2], **Nuria Benavent**[1,2], **Rafael Borge**[2], **and Alfonso Saiz-Lopez**[1]

[1]Department of Atmospheric Chemistry and Climate, Institute of Physical Chemistry Rocasolano, CSIC, Madrid 28006, Spain
[2]Universidad Politécnica de Madrid, UPM, 28006 Madrid, Spain

Correspondence: Alfonso Saiz-Lopez (a.saiz@csic.es)

Received: 17 June 2020 – Discussion started: 15 July 2020
Revised: 12 February 2021 – Accepted: 15 February 2021 – Published: 17 April 2021

Abstract. Trace gases play a key role in the chemistry of urban atmospheres. Therefore, knowledge about their spatial distribution is needed to fully characterize air quality in urban areas. Using a new Multi-AXis Differential Optical Absorption Spectroscopy two-dimensional (MAXDOAS-2D) instrument, along with an inversion algorithm (bePRO), we report the first two-dimensional maps of nitrogen dioxide (NO_2) and nitrous acid (HONO) concentrations in the city of Madrid, Spain. Measurements were made during 2 months (6 May–5 July 2019), and peak mixing ratios of 12 and 0.7 ppbv (parts per billion by volume) for NO_2 and HONO, respectively, were observed in the early morning in the southern part of the downtown area. We found good general agreement between the MAXDOAS-2D mesoscale observations – which provide a typical spatial range of a few kilometers – and the in situ measurements provided by Madrid's air quality monitoring stations. In addition to vertical profiles, we studied the horizontal gradients of NO_2 in the surface layer by applying the different horizontal light path lengths in the two spectral regions included in the NO_2 spectral analysis: ultraviolet (UV, at 360 nm) and visible (VIS, 477 nm). We also investigate the sensitivity of the instrument to infer vertically distributed information on aerosol extinction coefficients and discuss possible future ways to improve the retrievals. The retrieval of two-dimensional distributions of trace gas concentrations reported here provides valuable spatial information for the study of air quality in the city of Madrid.

1 Introduction

Air pollution in urban areas has become a concern in our society because it represents a major risk to human health and the environment (WHO, 2019). Air quality is often expressed as the state of air pollution in terms of gaseous pollutant concentrations, as well as the size and number of particulate matter that may affect human health, ecosystems and climate (Monks et al., 2009). Integral understanding of air pollution requires knowledge about the sources, pollutants, chemical composition and spatial distribution and their transport phenomena in the atmosphere (EEA, 2019).

Madrid, Spain, has suffered from severe air pollution in recent years with episodes of large nitrogen dioxide (NO_2) and ozone (O_3) concentrations. In an effort to control and reduce high-pollution events, the local government has enforced some traffic restriction measures (Izquierdo et al., 2020) and has set up several in situ air quality monitoring stations over the city's metropolitan area. These in situ instruments – as of today – cannot measure some important trace gases present in the atmosphere, and their values are only representative of the immediate surrounding of the instruments and at surface level. There is therefore a need for mesoscale analysis (both horizontal and vertical in the order of 10 km) of urban air pollution that could complement the in situ measurements. With this aim, we have deployed a Multi AXis Differential Optical Absorption Spectroscopy (MAXDOAS) instrument for air pollution measurements in Madrid. MAXDOAS is a widely used technique for the detection of trace gases in the atmosphere, and it is

based on the wavelength-dependent absorption of scattered sunlight by atmospheric constituents (Platt and Stutz, 2008). In addition to routinely monitored species such as NO_2 and O_3, MAXDOAS provides mesoscale measurements of other trace gases that are relevant to understand atmospheric chemistry, such as nitrous acid (HONO), formaldehyde (HCHO) or glyoxal (CHOCHO). Over the past few years, we have reported trace gas measurements in Madrid using the MAXDOAS technique (Wang et al., 2016; Garcia-Nieto et al., 2018; Benavent et al., 2019), as well as pollutant trend analysis and chemical transport modeling (Borge et al., 2018; Cuevas et al., 2014; Saiz-Lopez et al., 2017).

For this work, a new two-dimensional MAXDOAS instrument (which will be described in Sect. 3 and will be hereafter referred to as MAXDOAS-2D) has been built, tested and set up to take continuous measurements in Madrid. This instrument represents a follow-up development to our previous one-dimensional instrument (MAXDOAS-1D; see Wang et al., 2016) that incorporates the capability of moving in the azimuthal dimension, therefore allowing the collection of spectra pointing at any angular direction. This additional capability allows for the measurement of both the horizontal and vertical trace gas (e.g., NO_2) distribution throughout the city and in turn the generation of two-dimensional maps of trace gas concentrations. Several works using two-dimensional MAXDOAS instruments have been carried out in recent years (e.g., Ortega et al., 2016; Yang et al., 2019; Schreier et al., 2020; Dimitropoulou et al., 2020). These studies were mostly focused on mapping the NO_2 distribution in urban environments and assessing its role for air quality monitoring.

Here we present 2 months of MAXDOAS-2D measurements of scattered sunlight spectra. The measurements were taken from 6 May to 5 July 2019 with a focus on the evaluation of NO_2 vertical concentration profiles and the characterization of horizontal light path lengths. We also provide the retrieval of HONO as an example of the potential of the MAXDOAS-2D to provide spatial information also on other trace gases relevant to urban atmospheric chemistry. An assessment of the relation between the MAXDOAS data and the in situ measurements of NO_2 in the city was carried out. Section 2 provides details of the DOAS technique, while Sect. 3 describes the experimental setup. The inversion methods and the atmospheric parameters chosen for the analysis are detailed in Sect. 4. The two-dimensional NO_2 and HONO distributions, an evaluation of the light path geometries, along with their relative probabilities, and an assessment of horizontal mixing ratio gradients near the surface are discussed in Sect. 5.

2 Brief introduction to the DOAS method

The DOAS basic idea is described by the Beer–Lambert law which models the exponential attenuation of spectral irradiance when it traverses a certain sample that contains some absorbers:

$$I(\lambda, L) = I_0(\lambda) \exp\left(-\sum\nolimits_i \int_0^L \sigma_i(\lambda)\, \rho_i(s)\, \mathrm{ds}\right), \quad (1)$$

where λ is wavelength, σ_i and ρ_i stand for – respectively – the absorption cross section and concentration of a given absorber i along the path, and the pair I_0 and I represent the spectral irradiances at the beginning and end of the process under study. The absorption processes are integrated over the photon paths (with infinitesimal path ds) and summed over every present absorber (Platt and Stutz, 2008).

Specifically, the MAXDOAS technique is based on the study of the differential spectral absorption structures that are produced in the measured scattered sunlight spectra (Hönninger et al., 2004; Plane and Saiz-Lopez, 2006; Platt and Stutz, 2008). The main principle is based on identifying the narrowband absorption features within the measured optical density taking out the broadband optical density, mainly generated by Rayleigh and Mie scattering, as well as by instrumental effects. On the other hand, an analogous process is done on the trace gas absorption cross sections by means of filtering out the broadband spectral features, hence producing the so-called differential absorption cross sections which are unique for each trace gas, acting as their "fingerprints" and therefore enabling their specific detection.

For MAXDOAS, I_0 stands for the solar spectrum (known as the Fraunhofer spectrum with no Earth atmospheric absorptions), while I represents the recorded ground-based spectrum, which includes all the absorption and scattering processes. However, and since the actual photon path is difficult to determine with accuracy (see Sect. 4), the MAXDOAS calculations are done using relative absorptions between two different optical paths: a zenith spectrum that contains less absorptions and is assumed as a reference spectrum and another spectrum pointing to a given elevation angle. Therefore, the direct product of the method is the differential slant column density (DSCD), which can be defined as the difference in the integrated concentration of a given absorber between the two selected pointing directions (more details about the numerical procedure that lies behind can be found in Honninger et al., 2004; Plane and Saiz-Lopez, 2006, and Platt and Stutz, 2008). Finally, these DSCDs are used as the main input for the profile retrieval algorithms which simulate the state of the atmosphere with the purpose of reproducing the measured DSCDs. This final step yields the optimal vertical concentration profiles.

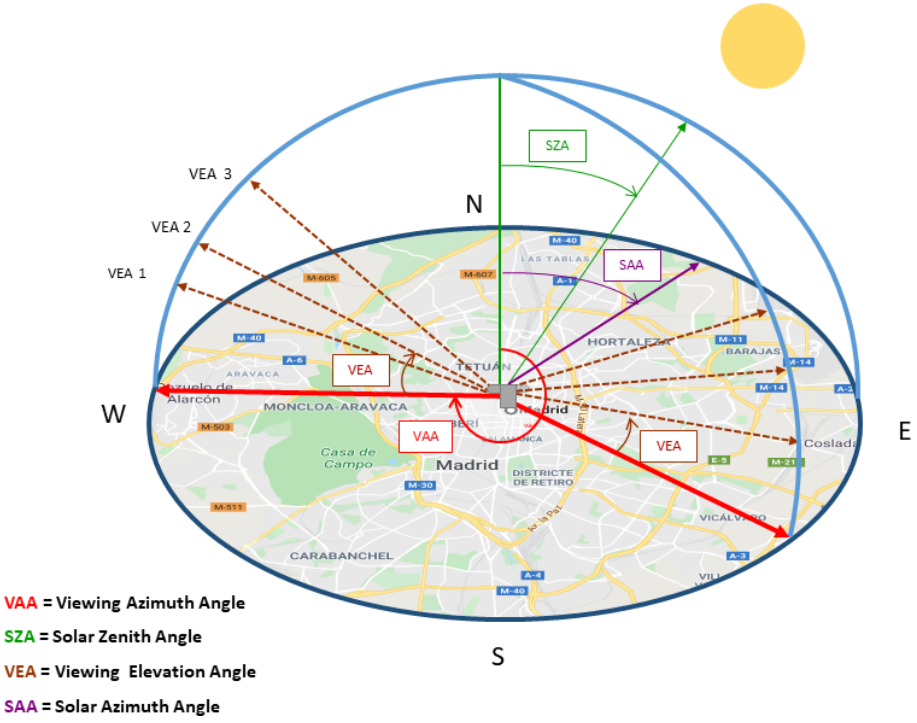

Figure 1. MAXDOAS-2D geometry diagram, the background of this picture represents the Madrid city center taken from © Google Maps.

3 Experiment

Briefly, MAXDOAS-1D instruments consist of a light collector attached to a stepper motor that scans the atmosphere at different viewing elevation angles (VEAs; see Fig. 1). The main feature added to the MAXDOAS-2D instrument is an additional stepper motor for the azimuthal movement, hence allowing the light collector to freely point to any angular direction in the atmosphere. This allows for the evaluation of trace gases absorptions for different viewing azimuth angles (VAAs; Fig. 1).

3.1 MAXDOAS-2D description

A MAXDOAS-2D instrument (Fig. 2) was built by the Atmospheric Chemistry and Climate group at the Institute of Physical Chemistry Rocasolano (IQFR-CSIC). Its main elements are based on our previous MAXDOAS-1D instrument: a light collector attached to a stepper motor, along with a focusing lens (80 mm focal length) are responsible for collecting the scattered sunlight. An Ocean Optics SMA 905 optical fiber of 1 m length conducts the light through an Ocean Optics HR4000 spectrometer (which incorporates a linear silicon charge-coupled device array as a detector). The spectrometer wavelength ranges roughly from 300 to 500 nm and offers an estimated spectral resolution (full width at half maximum) of about 0.5 nm. An additional stepper motor was included for azimuthal movement. The instrument incorporates all its components in an outdoor unit. Therefore, to maintain the spectrometer temperature as steady as possible – for both mechanical and wavelength calibration purposes – a Peltier cell was included. Additionally, a UPS device provides the power supply and eliminates possible strong power peaks. Two webcams take pictures of the cloud cover at each VAA and monitor the instrument itself. The instrument is autonomous, and it runs on homemade Java software. This software controls the movement, the spectrum collection and recording, and the surrounding accessories and automatically keeps it continuously measuring as long as the Sun is over the horizon.

3.2 Location

The MAXDOAS-2D instrument is located at the main campus of the Spanish National Research Council (CSIC) in Madrid, Spain. It is placed on the roof of the Instituto de Ciencias Agrarias (ICA) at a latitude of 40.4419° N and a longitude of 3.6875° W. The height of the building is approximately 70 m a.g.l (above ground level). This location in downtown Madrid can be classified as an urban site with the usual weather of continental areas at midlatitudes (i.e., hot and dry summers and cold winters) and with a prevalence of clear sky days during the year. NO_2 typically presents strong spatial concentration gradients in urban areas, and traffic hotspots have been reported in Madrid (Borge et al., 2016). This makes it difficult to clearly predict how NO_2 will be distributed; i.e., there is not a clear azimuthal direction preference for higher NO_2 at a certain time. However, mesoscale

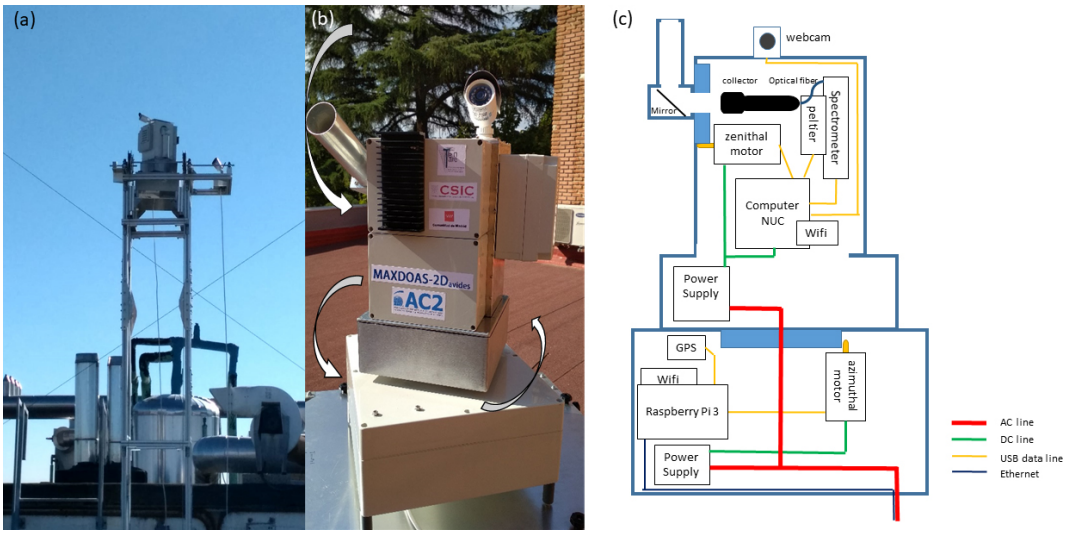

Figure 2. (a) Aluminum tower with the instrument installed on top of it; **(b)** MAXDOAS-2D instrument; **(c)** MAXDOAS-2D scheme.

simulations suggest that higher NO_2 mixing ratios can be expected in the southern part of Madrid, considering population distribution and commuting patterns (Picornell et al., 2019).

Due to some obstacles that blocked a clear view in some of the VAAs, a small aluminum tower was built to overcome the viewing obstacles, and the MAXDOAS-2D instrument was fixed on top of it (see Fig. 2). Once the instrument was set up, we aligned it for both angular movements – azimuthal and zenithal – with respect to the geographical north and the local horizontal (i.e., perpendicular to the gravitational plumb), respectively. This process was performed in two steps. First, the light collector was coarsely oriented using levels and a compass. Then, the alignment was refined doing a vertical scan of the Sun (which has a very well-known position vector) and its angular surroundings at several different times of a clear sky day. The angular differences between the measurements and the center of intensity of the registered spectra (a similar approach was done in Ortega et al., 2016) were estimated and the associated correction applied to the instrument.

3.3 Measurements setup

In order to sample and analyze a representative portion of the atmosphere over Madrid, selected angular directions were chosen. Starting at a VAA of 0° (pointing to the north), the MAXDOAS-2D rotated clockwise using steps of 20° in azimuth. In each azimuth direction, the ensuing VEA vector was used: 1, 2, 3, 5, 10, 30 and 90°. Therefore, an entire azimuthal lap was completed when the light collector was back again at a VAA of 0°.

For every measured spectrum, the spectrometer was able to correct for both electronic offset and dark current effects. Other important parameters for the measurements such as the integration time and the number of scans taken in each angular direction were automatically calculated. More specifically, for this study we set the goal of completing an azimuthal lap in approximately 1 h (mainly for an easier interpretation of the results and for the subsequent comparison with in situ instruments of Madrid's air quality monitoring network). Hence, we chose 24 s as the maximum exposure time in each angular combination.

The main advantage of this setup is that we can observe the daily NO_2 variability over the entire city with a moderate temporal resolution (1 h). The main disadvantage is that observations for each VAAs averaged over such a short integration period may be affected by microscale phenomena. Nonetheless, NO_2 concentration gradients are particularly strong in space (Borge et al., 2016). Therefore, this time resolution may be well suited to characterize both the azimuthal and the horizontal gradients of NO_2.

4 Analysis methods

The absorptions of the molecular oxygen dimer (O_4) and NO_2 were measured for the entire campaign and for two spectral windows: 352–387 nm (UV region) and 438–487 nm (VIS region). The analysis settings applied for the UV and VIS regions are summarized in Tables 1 and 2, respectively. These configurations mainly follow those used in Wagner et al. (2019).

The selected differential absorption cross sections – along with the spectral window and parameters included in Tables 1 and 2 – were adjusted to the measured differential optical density using the QDOAS spectral fitting software (http://uv-vis.aeronomie.be/software/QDOAS/, last access: October 2017). Figure 3 shows examples of the spectral detection of O_4 and NO_2 for both the UV and VIS regions.

Table 1. DOAS spectral settings for the retrieval of O_4 and NO_2 in the UV.

Parameter	Value
Fitting window	352–387 nm
Wavelength calibration	Based on reference solar atlas (Chance and Kurucz, 2010)
Zenith reference	Scan
Polynomial order	5
Intensity offset	Order 2
Shift	The measured spectra and ring were allowed to shift and stretch (order 1) in wavelength.
Molecule	Cross section
O_4	293 K (Thalman and Volkamer, 2013)
NO_2	298 K (Vandaele et al., 1998)
O_3_a	273 K (Serdyuchenko et al., 2014)
O_3_b	223 K (Serdyuchenko et al., 2014)
HCHO	297 K (Meller and Moortgat, 2000)
HONO	296 K (Stutz et al., 2000)
Ring_a	Calculated by QDOAS
Ring_b	Ring_a spectrum multiplied by λ^{-4}

Table 2. DOAS spectral settings for the retrieval of O_4 and NO_2 in the VIS.

Parameter	Value
Fitting window	438–487 nm
Wavelength calibration	Based on reference solar atlas (Chance and Kurucz, 2010)
Zenith reference	Scan
Polynomial order	5
Intensity offset	Order 2
Shift	The measured spectra and ring were allowed to shift and stretch (order 1) in wavelength.
Molecule	Cross section
O_4	293 K (Thalman and Volkamer, 2013)
NO_2	298 K (Vandaele et al., 1998)
O_3_a	273 K (Serdyuchenko et al., 2014)
O_3_b	223 K (Serdyuchenko et al., 2014)
H_2O	296 K (Rothman et al., 2010)
Glyoxal	296 K (Volkamer et al., 2005)
Ring_a	Calculated by QDOAS
Ring_b	Ring_a spectrum multiplied by λ^{-4}

4.1 Cloud-screening and quality filtering

The algorithms for MAXDOAS retrievals of trace gas vertical profiles are based on estimating the light paths (along with their corresponding scattering probability). A significant cloud cover could noticeably impact the calculations, mainly because of multiple scattering effects, adding large uncertainties to the retrieval process. For this reason, the set of measured spectra was cloud-screened using the cloud-free AERosol RObotic NETwork (AERONET) database. The AERONET databases are reported with three quality levels; in particular, we used the Level 2.0 (cloud-screened and quality-assured) database provided by the AERONET instrument in Madrid. This information is combined with the photos taken by the camera installed on the MAXDOAS. As mentioned in Sect. 3.1, this webcam points at the same azimuthal direction as the light collector. We estimated the cloud cover using a code that gets the RGB coordinates – the three chromatists of the blue, green and red – and changes them into LCh coordinates – L indicates lightness, C represents chroma, and h is the hue angle. Based on criteria of luminosity, color and saturation, the code estimates the cloud index (percentage of estimated cloud cover in a given azimuthal sky view). Filtering out cloudy skies with precision is rather challenging; therefore, we established a threshold to get as many clear sky views as possible. In order to do that, we first crossed our measured DSCDs with the AERONET 2.0 database, and subsequently, using the photos, we discarded the cycles taken with an estimated cloud index higher than 40 %.

In addition to cloud screening, several other quality filters were applied to the DSCDs. Firstly, every DSCD that

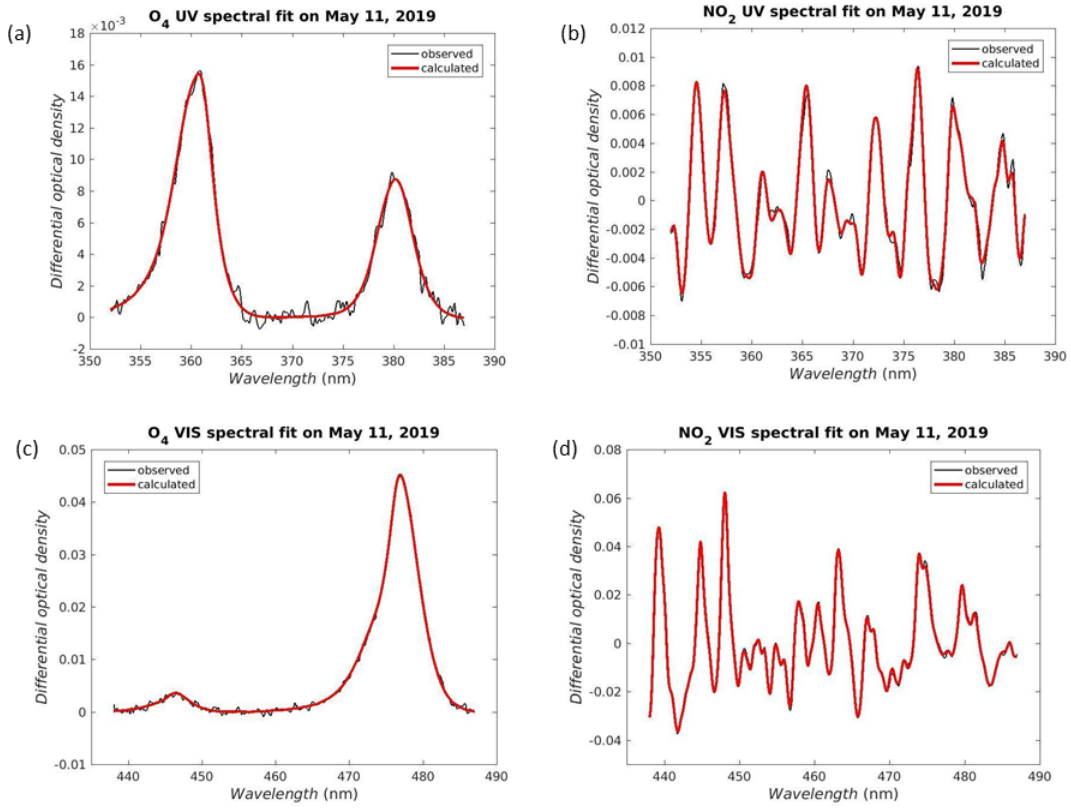

Figure 3. Spectral detection of O_4 **(a)** and **(c)** and NO_2 **(b)** and **(d)**. Red lines represent the calculated optical densities, and black lines are the measured optical densities. The viewing geometry of each detection was **(a)** VEA 2° and solar zenith angle, SZA, 26.4°, **(b)** VEA 3° and SZA 24.7°, **(c)** VEA 1° and SZA 22.6°, and **(d)** VEA 1° and SZA 48.7°.

yielded either a relative uncertainty larger than 1 or a residual root mean square (RMS) higher than 0.01 (in optical density units) was rejected. After that, we estimated the DSCD detection limit for a given trace gas as the ratio of the residual RMS (in optical density units) associated with each DSCD and the maximum value of the differential cross section of that trace gas. Then, we discarded the DSCDs that had an absolute value lower than twice the derived detection limit (a similar approach was carried out in Peters et al., 2012). Finally, we used the daily plus/minus 3 standard deviation criterion that AERONET applies for its cloud-filtered data, keeping the DSCD that falls within plus/minus 3 standard deviations from each daily mean.

4.2 Inversion algorithm and vertical profiles

An inversion algorithm method is applied to the measured DSCDs to estimate the light paths and subsequently derive the trace gas vertical concentration profile. For this work we have used the bePRO inversion algorithm (Clémer et al., 2010). The original calculation was built based on the optimal estimation method (OEM; Rodgers, 2000), and it comprises two steps: first, the light paths and the vertical profiles of irradiance extinction are calculated using the O_4 DSCDs; then, the target trace gas vertical concentration profile is retrieved using the corresponding light paths and measured absorption. In order to do that, bePRO simulates the atmospheric state characterizing several different physical phenomena including pressure and temperature vertical profiles, Rayleigh and Mie scattering events (along with their respective phase functions), the effect of the surface albedo, the light path geometries, and the irradiance extinction processes. Once the atmospheric vector state is defined, its combination with a certain vertical concentration profile results in the simulated DSCDs. This vertical profile is iterated until the generated set of simulated DSCDs is optimized with respect to the measured DSCDs so that the residual is minimized. As a result, an optimal vertical profile is obtained when the iteration is finished for each MAXDOAS cycle.

The measured O_4 DSCDs are used to estimate the light paths for each VEA since they are related to the square of the atmospheric O_2 profiles, which are well known. This profile is fairly steady during the day and does not heavily depend on chemistry factors. Therefore, the measured O_4 DSCDs can provide information on the irradiance extinction in the atmosphere. This extinction profile is usually associated with the aerosol extinction coefficients, and thus its vertical integration yields the aerosol optical depth (AOD). These aerosol

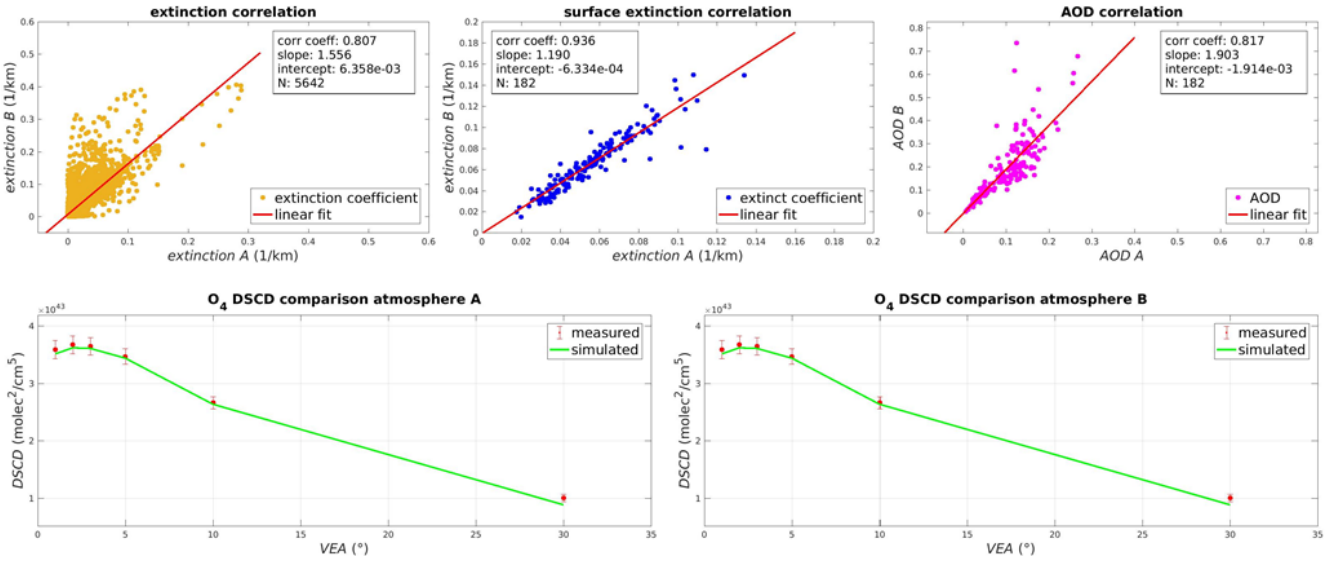

Figure 4. Comparison of retrieved aerosols using two different atmospheric profiles: the US standard (atmosphere A) and the US standard adapted to the altitude above sea level of Madrid (atmosphere B). The comparison was carried out for a clear sky day (11 May 2019).

extinction profiles are required to subsequently evaluate trace gas profiles since they strongly affect the relative light paths and hence the concentration profiles derived from them.

Once the light paths are computed, and with the purpose of best simulating the measured DSCDs, a linear analysis process is performed for the measured DSCDs of the target trace gas, yielding the optimal vertical concentration profile. The vertical integration of this concentration profile is called the vertical column density (VCD).

The retrieval consists of an iterative, nonlinear system of equations, and hence there is no unique solution. This means that an a priori profile is needed both for starting the iterations and to avoid the final solution being nonrealistic (i.e., with no physical meaning). In order to construct these a priori profiles, we used exponentially decreasing curves as follows:

$$\mathrm{ap}\,(z) = \frac{\mathrm{VC}_i}{\mathrm{sh}} \exp\left(\frac{-z}{\mathrm{sh}}\right), \tag{2}$$

where ap (z) is the a priori vertical profile at a certain altitude z, VC_i is the vertical integration of the profile for the MAXDOAS cycle i, and sh is the scaling height constant. We used 0.5 km as the scaling height constant for all the a priori profiles (Hendrick et al., 2014). Regarding the VC, we assumed an AOD of 0.05 for the O_4 retrieval, while for NO_2 we applied the geometrical approximation followed in Hönninger et al. (2004), taking the measured DSCD at VEA 30° for every MAXDOAS cycle. This approximation assumes that most of the absorption events are located below the scattering height.

With respect to the remaining atmospheric parameters, we chose typical values for urban environments: surface albedo of 0.07, correlation length of 0.4 km and an a priori covariance factor of 1 (see Hendrick et al., 2014). Concerning the vertical grid of the retrievals, we chose the following layers: from the ground to 8 km height we used layers of 200 m thickness. Then, we divided the remaining height, up to 90 km, in levels of 2 km thickness each. We use the air number density vertical profile since it is directly related to the number of O_4 absorptions and therefore to the O_4 DSCDs. Hence the relative differences, particularly for lower VEAs, between the measured and simulated O_4 DSCDs are usually assigned to aerosol extinction. Note, however, as shown below, that uncertainties in the air number density profiles – arising from uncertainties in the values or shape of the temperature and pressure profiles – could also contribute to such differences (Fig. 4).

Here we compare the simulation of O_4 DSCDs using two different sets of atmospheric profiles: (i) the US standard and (ii) the same profile but interpolating the pressure profile to Madrid's height above sea level (mean value of 667 m). This means that the temperature profile is assumed to be the same, but the pressure profile is shifted less than 10 %, so there are no major variations within the profiles. The lower row in Fig. 4 shows that both atmospheric profiles result in almost the same set of simulated O_4 DSCDs; however, the aerosol extinction coefficients differ significantly (although less for the surface layer coefficients, defined as the extinction coefficients within the ground layer, between 0 and 200 m height), and consequently, the AOD also varies. From this we infer the following.

i. The retrieval is mainly driven by the measured DSCDs, which leaves a relatively low weight for the chosen atmospheric profiles (pressure and temperature). Therefore, we can obtain consistent correlations between the measured and simulated O_4 DSCDs.

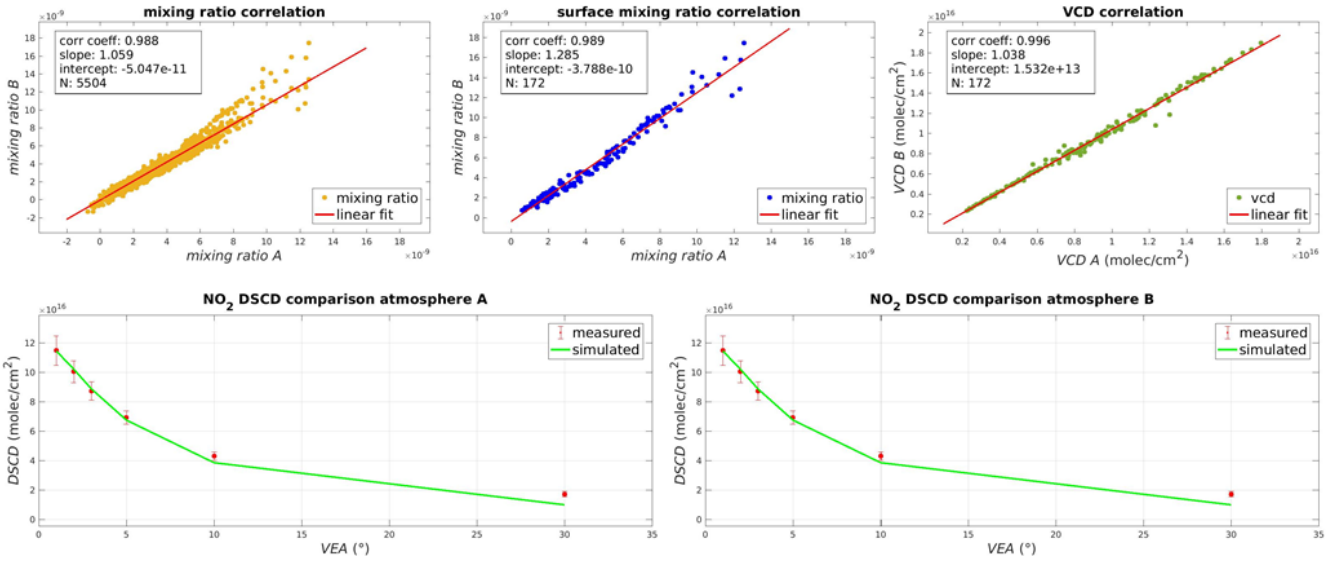

Figure 5. NO_2 retrieval comparison using two different atmospheric profiles: the US standard (atmosphere A) and the US standard adapted to the altitude above sea level of Madrid (atmosphere B). The comparison was carried out for a clear sky day (11 May 2019), considered as representative of the measurement period.

ii. We cannot reliably assign the extinction coefficients at each layer to aerosols (especially for atmospheric layers above the surface layer) but rather consider them as irradiance extinction coefficients.

Furthermore, we have assessed the impact of the pressure and temperature profile choice on the trace gas retrieval. As can be noted in Fig. 5, there is no significant effect coming from this choice on the simulated NO_2 DSCDs. These are basically the same (and with very good agreement with the measured DSCDs), as well as the derived concentration coefficients and their integration (VCD).

We further evaluated if a similar behavior can be expected for larger variations in the pressure and temperature profiles. We first obtained the average surface temperature and pressure values during the campaign (May–July 2019). With the inclusion of these values in the retrieval, we found that, within the first 10 km height, the RMS values of the relative variations with respect to the standard atmosphere were about 8 %. Although it is a small change, it is indeed not negligible. Nonetheless, when evaluating light paths, the relative changes were below 2 %. Therefore, here we use the US standard atmospheric profiles for the NO_2 retrievals.

Table 3 summarizes the average uncertainties (using 1 standard deviation for each component) of the retrieval, along with their relative contributions, for the ground layer (0–200 m height). The mean, overall uncertainty for NO_2 in both spectral regions is in the order of 10 %.

4.3 Estimation of NO_2 horizontal gradients

Making use of the different paths that photons travel through the atmosphere for different wavelengths, we can estimate

Table 3. Summary of average uncertainties of the retrieval in both spectral regions.

Variable/trace gas	NO_2 UV (%)	NO_2 VIS (%)
Irradiance extinction	7.7	5.1
DSCD	4.8	3.2
Surface mixing ratio	5.0	8.7
Total	10	11

the horizontal distribution of NO_2. We use the estimated horizontal light paths at two wavelengths, 360.8 and 477 nm, for the surface layer (0–200 m height). The different light paths at 360.8 and 477 nm provide information about the horizontal distribution of NO_2 mixing ratios within the surface layer. In order to evaluate these horizontal paths, we have a code that implements the radiative transfer model (RTM) equations based on previous pioneering work (Solomon et al., 1987). These equations yield a vector of scattering events along with their respective probabilities. If we take a VEA of 0° (i.e., horizontal viewing), then the scalar product of such vectors produces the length of the horizontal light path.

We computed this for every MAXDOAS cycle and for both wavelengths, yielding typical – representative – horizontal distances of about 8–10 km for the UV (at 360.8 nm) and between 15 and 20 km for the VIS window (at 477 nm). The next step follows the "onion-peeling" approach proposed by Ortega et al. (2016) (the strong dependence of scattering with wavelength means that shorter wavelengths result in shorter light paths). We assign the UV (i.e., 360.8 nm) mixing ratios (mr_{uv}) and their expected horizontal paths (d_{uv}) to

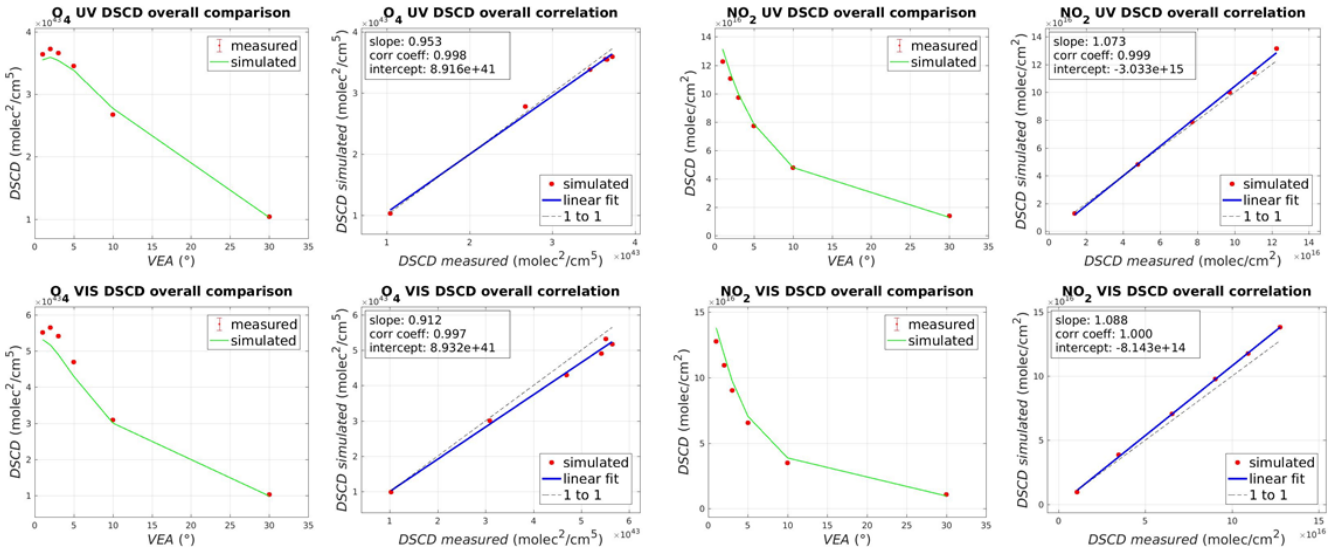

Figure 6. Comparison between simulated and measured DSCDs of O_4 and NO_2. Red dots represent the measured DSCDs for each VEA averaged over the entire campaign.

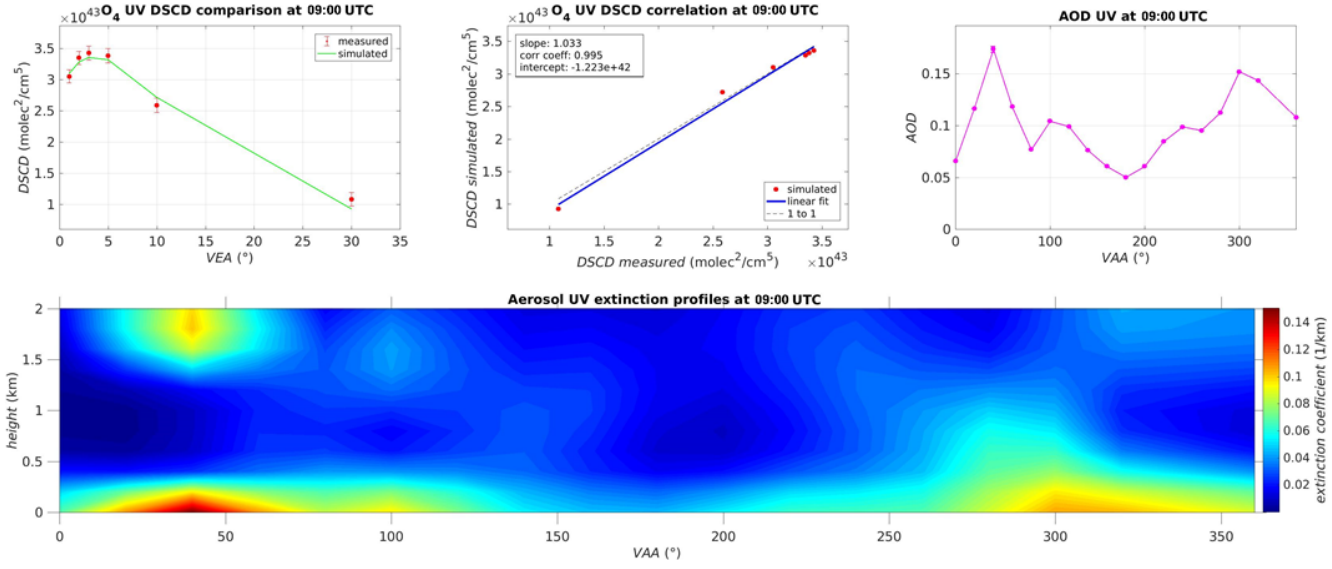

Figure 7. Example of O_4 and AOD retrievals in the UV region at 09:00 UTC on 11 May 2019. These contour plots are smoothed from adjacent VAA data points separated by 20° in order to estimate the azimuthal distribution of the irradiance extinction coefficients over Madrid.

the first peel (mr_A, meaning zone A). Then the second peel (zone B, mr_B) can be derived as follows:

$$mr_B = \frac{mr_{vis} \times d_{vis} - mr_{uv} \times d_{uv}}{d_{vis}}, \quad (3)$$

thereby deriving mixing ratios (mr_A and mr_B.) representative of two different horizontal distances for each VAA.

5 Results

5.1 O_4 and NO_2 DSCDs assessment

An estimation of the overall goodness of the profile retrieval comes from the correlation between the measured and simulated DSCDs for the entire campaign (Fig. 6). The fit between the measured and the simulated DSCDs shows correlations (r^2) very close to 1 for both O_4 and NO_2 in the UV and VIS regions.

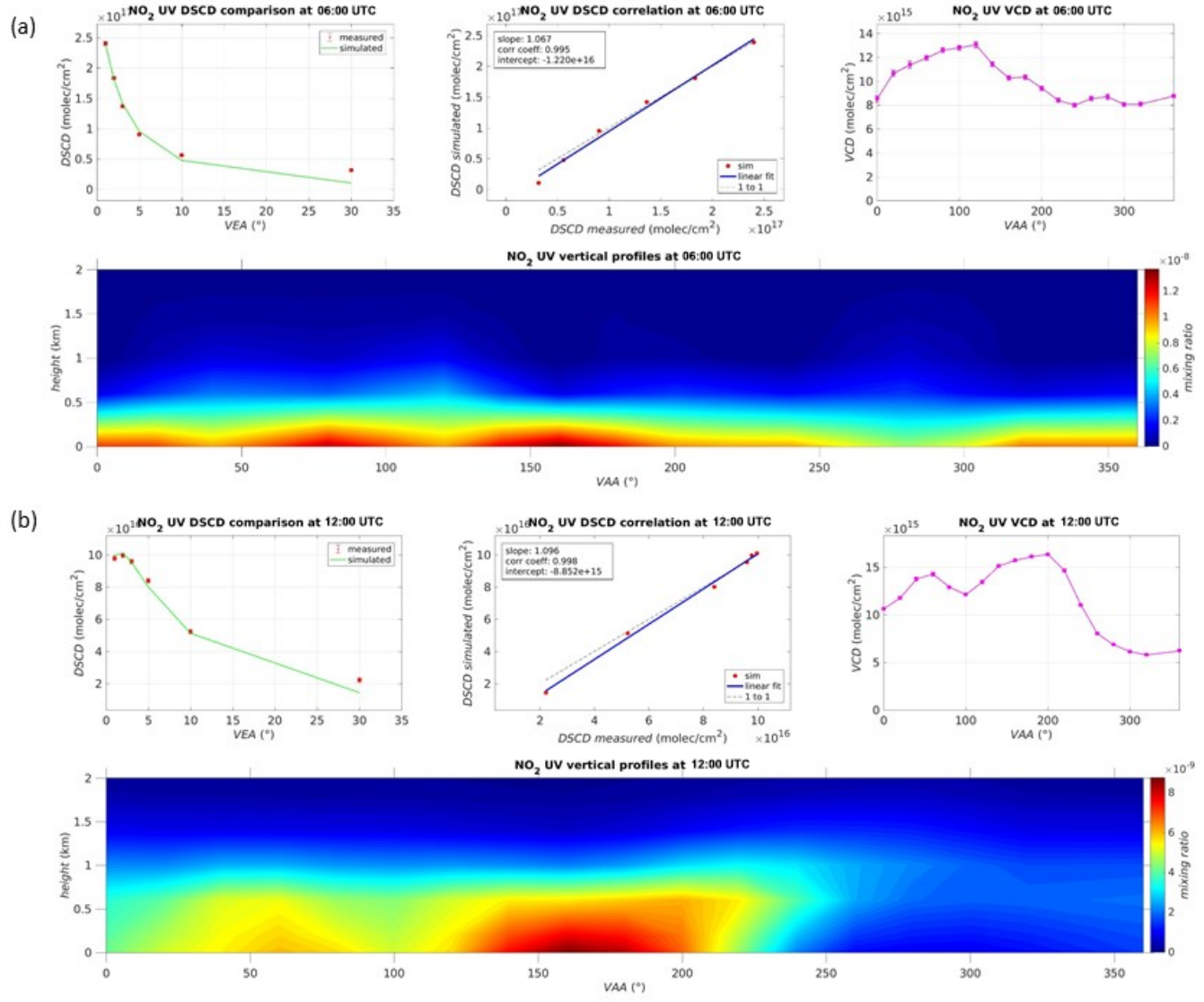

Figure 8. NO_2 vertical distribution retrieved in the UV region at 06:00 UTC **(a)** and at 12:00 UTC **(b)** on 11 May 2019. These contour plots are smoothed from adjacent VAA data points separated by 20° in order to estimate the azimuthal distribution of NO_2 over Madrid.

5.2 Two-dimensional maps

We now combine the VAA and height for each azimuthal cycle of the MAXDOAS-2D to generate a two-dimensional concentration map. Figure 7 shows an example of the O_4 retrieval in the UV for a given azimuthal cycle. Figure 7 also shows the comparison and correlation of measured and simulated DSCDs for that azimuthal cycle along with the evolution of retrieved AOD. The AOD varies between 0.05 and 0.18 within this azimuthal cycle (Fig. 7, upper panel). The contour plot shows the irradiance extinction coefficient profiles with maximum values of 0.14 km^{-1} (near the ground and at around 40° VAA) associated with aerosol extinction (see discussion in Sect. 4.2). Note the enhanced extinction at about 2 km height pointing at 50° VAA. This could be due to uplift of particulate matter emitted by traffic (there is a main road at that location) (Carnerero et al., 2018). Further research is needed to better establish the vertical distribution of aerosols in Madrid and their diurnal evolution.

Figure 8 shows a two-dimensional representation of NO_2 on 11 May 2019 at two different hours (06:00 and 12:00 UTC, respectively). Both contour plots show maximum NO_2 values of 12 ppbv (parts per billion by volume) at 06:00 UTC and 8 ppbv at 12:00 UTC when the instrument is pointing south (i.e., VAA of 180°). We chose to show this day as an example since it was a clear sky day and yielded NO_2 mixing ratios that were representative of the period of measurements. These values correspond to the layer near the ground and are in good agreement with our previous MAXDOAS observations in Madrid (Garcia-Nieto

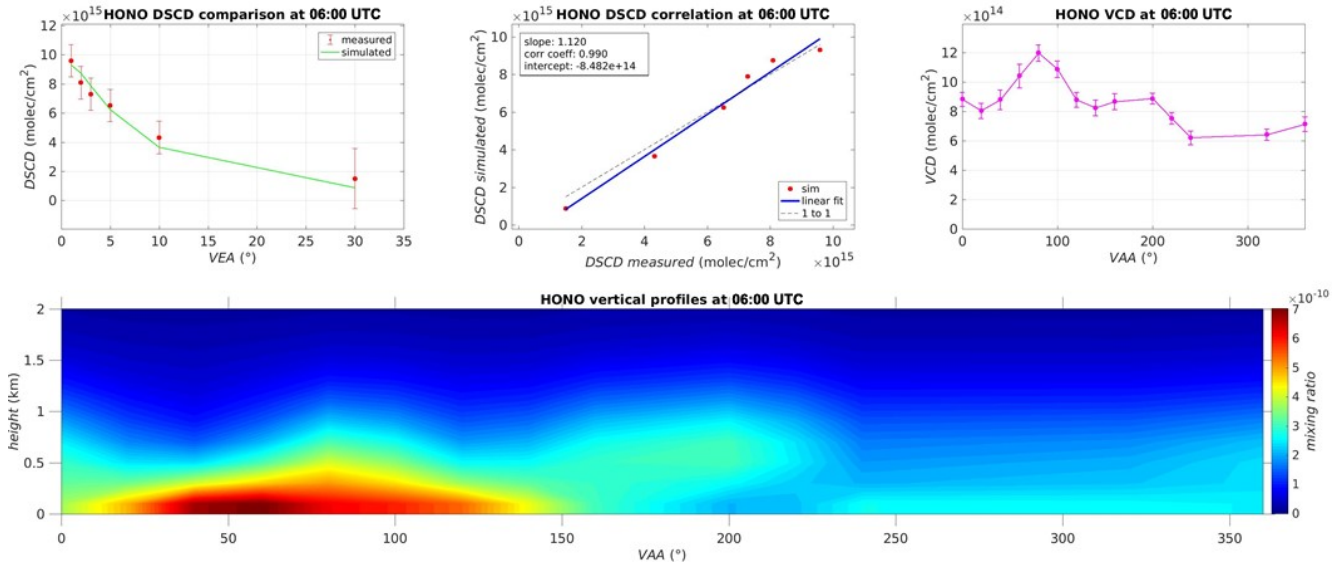

Figure 9. HONO vertical distribution retrieved in the UV region at 06:00 UTC. These contour plots are smoothed from adjacent VAA data points separated by 20° in order to estimate the azimuthal distribution of HONO over Madrid.

et al., 2018). The retrieved azimuthal distribution of NO_2 agrees with previous reports that show higher pollution levels in the southern part of Madrid (Picornell et al., 2019). NO_2 VCDs range from 5×10^{15} molec. cm^{-2} (at 12:00 UTC and pointing at 300° VAA) up to 15×10^{15} molec. cm^{-2} (at 12:00 UTC and pointing at 200° VAA), with an average value of 1×10^{16} molec. cm^{-2}. Although there are different NO_x emission rates at both times of the day (06:00 and 12:00 UTC), the increase in the boundary layer height (de la Paz et al., 2016) during the day contributes to the similar values of VCDs at both hours but generally lower surface mixing ratios at 12:00 UTC.

We have also analyzed HONO DSCDs using the same DOAS analysis configuration as in Garcia-Nieto et al. (2018). Figure 9 shows a two-dimensional representation of HONO on 11 May 2019 at 06:00 UTC. We retrieve surface layer peak values of 0.7 ppbv pointing at 50° VAA in the early morning, which is in agreement with previous studies for HONO in urban environments (see Hendrick et al., 2014; Ryan et al., 2018). The VCDs at 06:00 UTC range from 6×10^{14} to 1.2×10^{15} molec. cm^{-2}.

5.3 Horizontal distribution of NO_2

Based on Eq. (3), we derive the horizontal distribution of NO_2 in the surface layer (0–200 m height) using the measured NO_2 DSCDs at a VEA of 1° (which can safely be regarded as almost horizontal viewing since its mean scattering height typically falls below 200 m height, i.e., within our ground layer). Figure 10 shows an example of surface layer NO_2 mixing ratios over two radial distances horizontally measured from the MAXDOAS-2D instrument (using the UV and the VIS NO_2, respectively, as explained in Sect. 4.3), located at the center of the plot. The highest mixing ratios occur during the first sunlit hours (07:00–08:00 UTC), coincident with the morning peak of NO_x emissions in Madrid (Quaassdorff et al., 2016). This early morning peak is followed by a gradual decrease in surface layer NO_2 mixing ratios during the day. Note that NO_2 is predominantly located in the southern part of the semisphere (VAA from 90 to 270°). In follow up work we will combine the horizontal distribution of NO_2 with a chemical transport model to further understand NO_2 transport dynamics throughout the day.

5.4 Correlation with Madrid's in situ air quality monitoring stations

We suggest that MAXDOAS-2D mesoscale observations may complement the information provided by the local air quality monitoring network based on reference analytical techniques (according to Directive 2008/50/EC). While air quality monitors of the reference network provide information about ambient concentrations in their specific locations (currently 24 air quality monitoring stations measure NO_2 within the city; see AM, 2019), MAXDOAS-2D observations produce near-ground-level concentrations averaged over the optical path in a given direction. That prevents us from quantitatively comparing both types of observations. Nonetheless, we analyzed their correspondence using the NO_2 concentrations measured by the in situ instruments throughout the entire city and the NO_2 mixing ratios within the surface layer derived from our MAXDOAS-2D instrument over the 2-month period (May–June, 2019). For this comparison, we considered the air quality monitoring stations within a distance from the MAXDOAS-2D equal to or lower than 10 km (thus 20 air quality monitoring stations

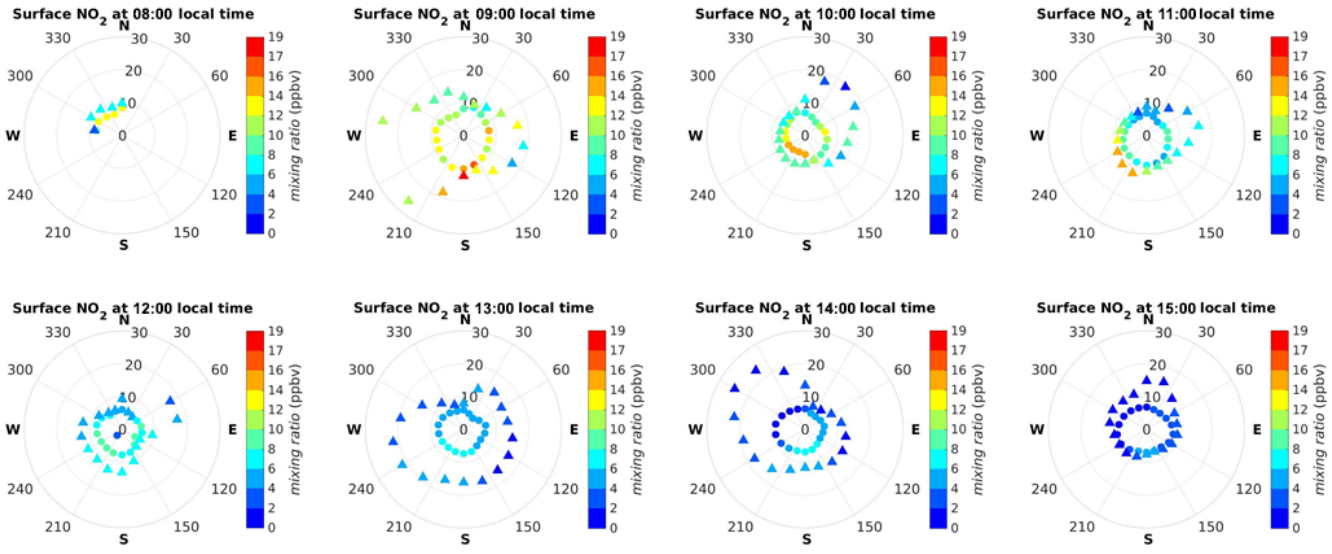

Figure 10. Polar plots of NO_2 within the surface layer (0–200 m height) for 11 May 2019. Please note that these polar plots extend over a direction perpendicular to those shown in Fig. 8. Here, circles are used for the UV (shorter horizontal light path) and triangles for the VIS (larger horizontal light path). Both symbols stand for the mean horizontal light path within the surface layer at each spectral region.

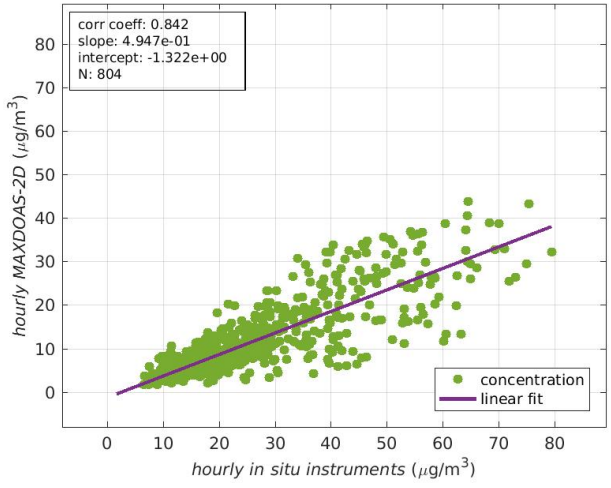

Figure 11. Correlation between in situ observations from Madrid's air quality monitoring network and those derived from the MAXDOAS-2D instrument for the surface layer (0–200 m height).

remain). Since this is the typical horizontal light path for the UV region, we decided to include only the NO_2 values retrieved in the UV region for the comparison. Strong gradients between the values measured by the in situ instruments are typical. Therefore, and considering that we are mainly interested in their temporal correlation with respect to our measurements, we compare both the in situ NO_2 and surface layer MAXDOAS-2D hourly averaged data. Note that for the MAXDOAS-2D, this approximately corresponds to averaging the surface layer values for each azimuthal lap, given that each azimuthal lap takes approximately 1 h to complete.

Despite the different spatial representativeness, Fig. 11 shows a reasonably good correlation coefficient of 0.842 between both datasets for the 2-month campaign. The slope is lower than 1; this can be explained by the typical NO_2 vertical profiles in urban environments. Simulations performed over Madrid with a high-resolution Eulerian air quality model (Borge et al., 2018) yielded a NO_2 profile exponentially decreasing with height. Therefore, the MAXDOAS-2D mixing ratios, which represent an average across the surface layer (0–200 m height), are not expected to quantitatively match the values of in situ instruments located close to the surface (between 0–10 m height). Similar conclusions – and slopes comparable to the one retrieved above – regarding the correlation between in situ and MAXDOAS instruments can be found in previous works (Schreier et al., 2020; Kramer et al., 2008; Chan et al., 2020). In addition, there is a good temporal correlation between in situ and MAXDOAS-2D measurements over an extended period of time.

6 Summary and conclusions

An analysis of O_4, NO_2 and HONO vertical concentration profiles in the urban atmosphere of Madrid (Spain) has been performed over 2 months (from 6 May to 5 July 2019). We analyzed the absorptions and derived the corresponding DSCDs for both trace gases in the UV and VIS regions. Then, the corresponding profiles were retrieved using an RTM. In this step, we assessed the impact of different atmospheric profiles (pressure and temperature) in the retrieval results and found that the set of chosen atmospheric profiles has a small impact on the O_4 retrieval and the estimation of light paths. However, there is a noticeable change in the irradiance ex-

tinction profiles which makes it difficult to quantitatively assign extinction due to aerosols, especially in heights above the boundary layer.

The overall comparison of measured and simulated trace gas DSCDs showed that they were in very good agreement (with correlation coefficients close to 1), supporting the reliability of the observations. The MAXDOAS-2D instrument provides the first two-dimensional view (in height and VAA) of pollution concentration in the city of Madrid. Exploring 1 d (11 May 2019) we compared two hours: the peak rush hour and noon time, obtaining NO_2 maximum values of 12 and 8 ppbv, respectively, both maxima pointing in the southern direction. Two-dimensional HONO measurements were also made with mixing ratio peaks of 0.7 ppbv in the early morning and VCDs ranging from 6×10^{14} to 1.2×10^{15} molec. cm^{-2}.

We have also inferred information on the horizontal gradient of NO_2 within the surface layer making use of the strong dependence between wavelengths and light paths across the NO_2 absorption spectrum. The resulting "onion-peeling" figures indicate peak values of NO_2 in the early morning and in the southern section of the city (around 180° VAA), and it resulted in a gradual decrease in NO_2 mixing ratios during the day, with maximum values of NO_2 appearing in the southern part of the semisphere. Finally, we suggest that the new mesoscale information provided by the MAXDOAS-2D instrument helps in the study of pollution transport dynamics. MAXDOAS-2D and in situ instruments provide different information, and thus combining both can improve our understanding of the complex issue of air pollution in the city of Madrid.

Code availability. The DOAS software and bePRO inversion algorithm used for this study are available at http://uv-vis.aeronomie.be/software (last access: 2 September 2017, Danckaert et al., 2017), while the RTM codes applied to derive the light paths are available upon request.

Data availability. All study data are included in the article.

Author contributions. ASL devised the research. DGN and NB carried out the measurements and analyzed the data. DGN, NB, RB and ASL analyzed and interpreted the results. DGN wrote the manuscript with contributions from all coauthors.

Competing interests. The authors declare that they have no conflict of interest.

Acknowledgements. The authors want to thank Manuel Perez and David Armenteros for technical assistance with the instrument and David de la Paz for model assistance. This work was supported by the TECNAIRE project ("Técnicas innovadoras para la evaluación y mejora de la calidad del aire urbano") S2013/MAE-2972. We would also like to thank Juan Ramón Moreta González (PI) and his staff for establishing and maintaining the AERONET sites in Madrid used in this investigation. We acknowledge support of the publication fee by the CSIC Open Access Publication Support Initiative through its Unit of Information Resources for Research (URICI)

Financial support. This research has been supported by the TECNAIRE PROJECT (grant no. S2013/mae-2972).

We acknowledge support of the publication fee by the CSIC Open Access Publication Support Initiative through its Unit of Information Resources for Research (URICI).

Review statement. This paper was edited by Daniel Perez-Ramirez and reviewed by three anonymous referees.

References

Ayuntamiento de Madrid (AM): Madrid 2016 Annual Air Quality Assessment Report (Calidad del aire Madrid 2019), General Directorate of Sustainability and Environmental Control, Madrid City Council Available online, only Spanish version, available at: http://www.mambiente.munimadrid.es/opencms/calaire/Publicaciones/memoria_2019.html (last access: April 2020), 2019.

Benavent, N., Garcia-Nieto, D., Wang, S., and Saiz-Lopez, A.: MAX-DOAS measurements and vertical profiles of glyoxal and formaldehyde in Madrid, Spain, Atmos. Environ., 199, 357–367, 2019.

Borge, R., Narros, A., Artínano, B., Yagüe, C., Gómez-Moreno, F. J., Paz, D. d. l., Román-Cascón, C., Díaz, E., Maqueda, G., Sastre, M., and Quaassdorff, C., Dimitroulopoulou, C., Vardoulakis, S.: Assessment of micro-scale spatio-temporal variation of air pollution at an urban hotspot in Madrid (Spain) through an extensive field campaign, Atmos. Environ., 140, 432–445, 2016.

Borge, R., Santiago, J. L., de la Paz, D., Martín, F., Domingo, J., Valdés, C., Sánchez, B., Rivas, E., Rozas, M. T., Lázaro, S., Pérez, J., and Fernández, Á.: Application of a short term air quality action plan in Madrid (Spain) under a high-pollution episode – Part II: Assessment from multi-scale modelling, Sci. Total Environ., 635, 1574–1584, https://doi.org/10.1016/j.scitotenv.2018.04.323, 2018.

Carnerero, C., Pérez, N., Reche, C., Ealo, M., Titos, G., Lee, H.-K., Eun, H.-R., Park, Y.-H., Dada, L., Paasonen, P., Kerminen, V.-M., Mantilla, E., Escudero, M., Gómez-Moreno, F. J., Alonso-Blanco, E., Coz, E., Saiz-Lopez, A., Temime-Roussel, B., Marchand, N., Beddows, D. C. S., Harrison, R. M., Petäjä, T., Kulmala, M., Ahn, K.-H., Alastuey, A., and Querol, X.: Vertical and horizontal distribution of regional new particle formation events in Madrid, Atmos. Chem. Phys., 18, 16601–16618, https://doi.org/10.5194/acp-18-16601-2018, 2018.

Chan, K. L., Wiegner, M., van Geffen, J., De Smedt, I., Alberti, C., Cheng, Z., Ye, S., and Wenig, M.: MAX-DOAS measurements of tropospheric NO_2 and HCHO in Munich and the

comparison to OMI and TROPOMI satellite observations, Atmos. Meas. Tech., 13, 4499–4520, https://doi.org/10.5194/amt-13-4499-2020, 2020.

Chance, K. and Kurucz, R. L.: An improved high-resolution solar reference spectrum for earth's atmosphere measurements in the ultraviolet, visible, and near infrared, Special Issue Dedicated to Laurence S. Rothman on the Occasion of his 70th Birthday 111, J. Quant. Spectrosc. Ra., 9, 1289–1295, 2010.

Clémer, K., Van Roozendael, M., Fayt, C., Hendrick, F., Hermans, C., Pinardi, G., Spurr, R., Wang, P., and De Mazière, M.: Multiple wavelength retrieval of tropospheric aerosol optical properties from MAXDOAS measurements in Beijing, Atmos. Meas. Tech., 3, 863–878, https://doi.org/10.5194/amt-3-863-2010, 2010.

Cuevas, C., Notario, A., Adame, J., Hilboll, A., Richter, A., Burrows, J. P, and Saiz-Lopez, A.: Evolution of NO_2 levels in Spain from 1996 to 2012, Sci. Rep., 4, 5887, https://doi.org/10.1038/srep05887, 2014.

Danckaert, T., Fayt, C., Van Roozendael, M., De Smedt, I., Letocart, V., Merlaud, A., and Pinardi, G.: QDOAS Software user manual, Belgian Institute for Space Aeronomy, available at: https://uv-vis.aeronomie.be/software/QDOAS/QDOAS_manual.pdf, last access: 2 September 2017.

de la Paz, D., Borge, R., and Martilli, A.: Assessment of a high resolution annual WRF-BEP/CMAQ simulation for the urban area of Madrid (Spain), Atmos. Environ., 144, 282–296, https://doi.org/10.1016/j.atmosenv.2016.08.082, 2016.

Dimitropoulou, E., Hendrick, F., Pinardi, G., Friedrich, M. M., Merlaud, A., Tack, F., De Longueville, H., Fayt, C., Hermans, C., Laffineur, Q., Fierens, F., and Van Roozendael, M.: Validation of TROPOMI tropospheric NO_2 columns using dual-scan multi-axis differential optical absorption spectroscopy (MAX-DOAS) measurements in Uccle, Brussels, Atmos. Meas. Tech., 13, 5165–5191, https://doi.org/10.5194/amt-13-5165-2020, 2020.

European Environment Agency (EEA): Air quality in Europe – 2019 report, EEA Technical Report No 10/2019, ISBN: 978-92-9480-088-6, available at: https://www.eea.europa.eu/publications/air-quality-in-europe-2019 (last access: May 2020), 2019.

Hendrick, F., Müller, J.-F., Clémer, K., Wang, P., De Mazière, M., Fayt, C., Gielen, C., Hermans, C., Ma, J. Z., Pinardi, G., Stavrakou, T., Vlemmix, T., and Van Roozendael, M.: Four years of ground-based MAX-DOAS observations of HONO and NO2 in the Beijing area, Atmos. Chem. Phys., 14, 765–781, https://doi.org/10.5194/acp-14-765-2014, 2014.

Garcia-Nieto, D., Benavent, N., and Saiz-Lopez, A.: Measurements of atmospheric HONO vertical distribution and temporal evolution in Madrid (Spain) using the MAXDOAS technique, Sci. Total Environ., 643, 957–966, 2018.

Gorshelev, V., Serdyuchenko, A., Weber, M., Chehade, W., and Burrows, J. P.: High spectral resolution ozone absorption cross-sections – Part 1: Measurements, data analysis and comparison with previous measurements around 293 K, Atmos. Meas. Tech., 7, 609–624, https://doi.org/10.5194/amt-7-609-2014, 2014.

Hönninger, G., von Friedeburg, C., and Platt, U.: Multi axis differential optical absorption spectroscopy (MAX-DOAS), Atmos. Chem. Phys., 4, 231–254, https://doi.org/10.5194/acp-4-231-2004, 2004.

Izquierdo, R., García Dos Santos, S., Borge, R., Paz, D. de la, Sarigiannis, D., Gotti, A., and Boldo, E.: Health impact assessment by the implementation of Madrid City air-quality plan in 2020, Environ. Res., 183, 109021, https://doi.org/10.1016/j.envres.2019.109021, 2020.

Kramer, L. J., Leigh, R. J., Remedios, J. J., and Monks, P. S: Comparison of OMI and ground-based in situ and MAX-DOAS measurements of tropospheric nitrogen dioxide in an urban area, J. Geophys. Res.-Atmos., 113, D16S39, https://doi.org/10.1029/2007JD009168, 2008.

Meller, R. and Moortgat, G. K.: Temperature dependence of the absorption cross sections of formaldehyde between 223 and 323 K in the wavelength range 225–375 nm, J. Geophys. Res.-Atmos., 105, 7089–7101, 2000.

Monks, P. S., Granier, C., Fuzzi, S., Stohl, A., Williams, M. L., Akimoto, H., Amann, M.,Baklanov, A., Baltensperger, U., Bey, I., Blake, N., Blake, R. S., Carslaw, K., Cooper, O. R., Dentener, F., Fowler, D., Fragkou, E., Frost, G. J., Generoso, S., and von Glasow, R.: Atmospheric composition change – global and regional air quality, Atmos. Environ., 43, 5268–5350, https://doi.org/10.1016/j.atmosenv.2009.08.021, 2009.

Ortega, I., Coburn, S., Berg, L. K., Lantz, K., Michalsky, J., Ferrare, R. A., Hair, J. W., Hostetler, C. A., and Volkamer, R.: The CU 2-D-MAX-DOAS instrument – Part 2: Raman scattering probability measurements and retrieval of aerosol optical properties, Atmos. Meas. Tech., 9, 3893–3910, https://doi.org/10.5194/amt-9-3893-2016, 2016.

Peters, E., Wittrock, F., Großmann, K., Frieß, U., Richter, A., and Burrows, J. P.: Formaldehyde and nitrogen dioxide over the remote western Pacific Ocean: SCIAMACHY and GOME-2 validation using ship-based MAX-DOAS observations, Atmos. Chem. Phys., 12, 11179–11197, https://doi.org/10.5194/acp-12-11179-2012, 2012.

Picornell, M., Ruiz, T., Borge, R., García-Albertos, P., de la Paz, D., and Lumbreras, J.: Population dynamics based on mobile phone data to improve air pollution exposure assessments, J. Expo. Sci. Environ. Epidemiol., 29, 278–291, https://doi.org/10.1038/s41370-018-0058-5, 2019.

Plane, J. M. C. and Saiz-Lopez, A.: UV-Visible Differential Optical Absorption Spectroscopy (DOAS), in: Analytical Techniques for Atmospheric Measurement, edited by: Heard, D. E., Blackwell Publishing, Oxford, 553 pp., 2006.

Platt, U. and Stutz, J.: Differential Optical Absorption Spectroscopy: Principles and Applications, Springer Berlin Heidelberg, Berlin, Heidelberg, 608 pp., 2008.

Quaassdorff, C., Borge, R., Pérez, J., Lumbreras, J., de la Paz, D., and de Andrés, J. M.: Microscale traffic simulation and emission estimation in a heavily trafficked roundabout in Madrid (Spain), Sci. Total Environ., 566, 416–427, https://doi.org/10.1016/j.scitotenv.2016.05.051, 2016.

Rodgers, C. D.: Inverse Methods for Atmospheric Sounding: Theory and Practice, World Scientific Publishing, Singapore, 256 pp., 2000.

Rothman, L. S., Gordon, I. E., Barber, R. J., Dothe, H., Gamache, R. R., Goldman, A., Perevalov, V. L., Tashkum, S. A., and Tennyson, J.: HITEMP, the high-temperature molecular spectroscopic database, J. Quant. Spectrosc. Ra. 111, 2139, https://doi.org/10.1016/j.jqsrt.2010.05.001, 2010.

Ryan, R. G., Rhodes, S., Tully, M., Wilson, S., Jones, N., Frieß, U., and Schofield, R.: Daytime HONO, NO_2 and aerosol distributions from MAX-DOAS observations in Melbourne, Atmos.

Chem. Phys., 18, 13969–13985, https://doi.org/10.5194/acp-18-13969-2018, 2018.

Saiz-Lopez, A., Borge, R., Notario, A., Adame, J. A., Paz, D., Querol, X., Artíñano, B., Gómez-Moreno, F. J., and Cuevas, C. A.: Unexpected increase in the oxidation capacity of the urban atmosphere of Madrid, Spain, Sci. Rep., 7, 45956, https://doi.org/10.1038/srep45956, 2017.

Schreier, S. F., Richter, A., Peters, E., Ostendorf, M., Schmalwieser, A. W., Weihs, P., and Burrows, J. P: Dual ground-based MAX-DOAS observations in Vienna, Austria: Evaluation of horizontal and temporal NO_2, HCHO, and CHOCHO distributions and comparison with independent data sets, Atmos. Environ., 5, https://doi.org/10.1016/j.aeaoa.2019.100059, 2020.

Solomon, S., Sanders, R. W., and Schmeltekopf, A. L.: On the Interpretation of Zenith Sky Absorption Measurements, J. Geophys. Res., 92, 8311–8319, 1987.

Stutz, J., Kim, E. S., Platt, U., Bruno, P., Perrino, C., and Febo, A.: UV-visible absorption cross sections of nitrous acid, J. Geophys. Res.-Atmos., 105, 14585–14592, 2000.

Thalman, R. and Volkamer, R.: Temperature dependent absorption cross-sections of O_2-O_2 collision pairs between 340 and 630 nm and at atmospherically relevant pressure, Phys. Chem. Chem. Phys., 15, 15371–15381, 2013.

Vandaele, A. C., Hermans, C., Simon, P. C., Carleer, M., Colin, R., Fally, S., Mérienne, M. F., Jenouvrier, A., and Coquart, B.: Measurements of the NO_2 absorption cross-section from $42\,000\,cm^{-1}$ to $10\,000\,cm^{-2}$ (238–1000 nm) at 220 K and 294 K, J. Quant. Spectrosc. Ra., 59, 171–184, 1998.

Volkamer, R., Spietz, P., Burrows, J., and Platt, U.: High-resolution absorption cross-section of glyoxal in the UV-vis and IR spectral ranges, J. Photochem. Photobiol. Chem., 172, 35–46, 2005.

Wagner, T., Beirle, S., Benavent, N., Bösch, T., Chan, K. L., Donner, S., Dörner, S., Fayt, C., Frieß, U., García-Nieto, D., Gielen, C., González-Bartolome, D., Gomez, L., Hendrick, F., Henzing, B., Jin, J. L., Lampel, J., Ma, J., Mies, K., Navarro, M., Peters, E., Pinardi, G., Puentedura, O., Puķıte, J., Remmers, J., Richter, A., Saiz-Lopez, A., Shaiganfar, R., Sihler, H., Van Roozendael, M., Wang, Y., and Yela, M.: Is a scaling factor required to obtain closure between measured and modelled atmospheric O_4 absorptions? An assessment of uncertainties of measurements and radiative transfer simulations for 2 selected days during the MAD-CAT campaign, Atmos. Meas. Tech., 12, 2745–2817, https://doi.org/10.5194/amt-12-2745-2019, 2019.

Wang, S., Cuevas, C. A., Frieß, U., and Saiz-Lopez, A.: MAX-DOAS retrieval of aerosol extinction properties in Madrid, Spain, Atmos. Meas. Tech., 9, 5089–5101, https://doi.org/10.5194/amt-9-5089-2016, 2016.

World Health Statistics (WHO): monitoring health for the SDGs, Wold Health Organization, available at: https://apps.who.int/iris/handle/10665/324835 (last access: May 2020), 2019.

Yang, T., Si, F., Luo, Y., Zhan, K., Wang, P., Zhou, H., Zhao, M., and Liu, W.: Source contribution analysis of tropospheric NO_2 based on two-dimensional MAX-DOAS measurements, Atmos. Environ., 210, 186–197, 2019.